BS 2019 2-4 SEPT ROME 16th IBPSA INTERNATIONAL CONFERENCE AND EXHIBITION

INTERNATIONAL BUILDING PERFORMANCE SIMULATION ASSOCIATION

Dehumidification Performance Improvement of a Cross-Flow Liquid Desiccant Dehumidifier through Physical Dimensions Modification

Hye-Jin Cho[1], Beom-Jun Kim[1], Soo-Jin Lee[1], and Jae-Weon Jeong[1]
[1] Department of Architectural Engineering, Hanyang University, Seoul, Republic of Korea

Abstract

The configuration of the dehumidifier plays an important role in the dehumidification performance of the liquid desiccant system. In this study, a parametric analysis of each geometric parameter on dehumidification performance was conducted to investigate the dehumidifier configuration for improving the dehumidification performance of a cross-flow liquid desiccant dehumidifier. To analyze the effects of the geometrical parameters (i.e., packing height, length, width, and air/solution side aspect ratio) on dehumidification performance, the air-desiccant contacting area estimation method and a two-dimensional heat and mass transfer numerical model was adopted. Two performance indices, the dehumidification effectiveness and pressure drop, were calculated via a series of simulations. Based on the simulation process, parametric analysis of each geometrical parameter on dehumidification performance were conducted. From the parametric analysis conducted using the proposed numerical model, it is clear that the solution side mass transfer area has a more significant effect on the dehumidification performance compared with that of the air side. In addition, increasing the packing length achieves higher dehumidification effectiveness compared with increasing the packing width. Consequently, it may be concluded that the cross-flow liquid desiccant dehumidifier can have a high dehumidification performance comparable to that of the counter-flow dehumidifier, achieved by modifying the physical dimensions of the packing tower, especially the packing length.

Introduction

In recent years, the liquid desiccant-based dehumidification system has been considered as a promising dehumidification technology alternative to the conventional vapor compression air conditioning systems (Goetzler et al., 2014). Desiccant-based dehumidification systems are driven by the vapor pressure difference between the process air and the desiccant solution. In dehumidification process, the process air flows into the dehumidifier tower, while the strong desiccant solution is sprayed on the packing media. When the incoming air contacts the packing media which is sufficiently wetted by the strong desiccant solution, the coupled heat and mass transfer process occurs immediately between the process air and desiccant solution.

In a liquid desiccant dehumidifier, the dehumidifier configuration has a significant impact on dehumidification performance. The flow direction of the process air and the desiccant solution (i.e., counter-flow, parallel-flow, and cross-flow) is one of the main concerns for designing the liquid desiccant dehumidifier. A counter-flow is the most widely adopted flow type because it has a relatively higher dehumidification ability compared with other flow types. However, the carryover of the liquid desiccant occurs severely in a counter-flow liquid desiccant dehumidifier as the process air takes up many droplets of the desiccant solution when the process air and desiccant solution flow along the same axis. Therefore, the carryover in a counter-flow liquid desiccant dehumidifier is considered as a major problem affecting indoor air quality (Fu and Liu, 2017). Furthermore, the packing height of a counter-flow dehumidifier tower could be limited in some building applications owing to limitations in available floor height. Thus, recent studies have focused on the cross-flow liquid desiccant dehumidifiers because they could mitigate some problems, such as solution carryover and installation difficulties due to limited floor height in building applications.

To compare the dehumidification performance of the counter-flow and cross-flow liquid desiccant dehumidifiers in equal physical sizes under identical operating conditions, a previous study conducted experiments in an environmental test chamber (Cho et al., 2018). From the experiment's results, it was observed that the cross-flow liquid desiccant dehumidifier has a relatively stable dehumidification performance regardless of the change of operating parameters. However, the cross-flow liquid desiccant dehumidifier showed limited dehumidification performance at higher inlet air humidity ratio compared with that of the counter flow type. Therefore, it is necessary to investigate ways to improve the dehumidification performance of the cross-flow dehumidifier to obtain the comparable to that of the counter-flow dehumidifier even in humid conditions.

The air-desiccant contacting area also plays an important role in the dehumidification performance of the liquid desiccant dehumidifier (Mei and Dai, 2008). The air-desiccant contacting area can be enlarged by increasing the geometrical parameters of the dehumidifier tower (i.e., packing height, length, and width).

https://doi.org/10.26868/25222708.2019.210886

Consequently, this study carried out a parametric analysis of each geometrical parameter on dehumidification performance to investigate the dehumidifier configuration for performance improvement in a cross-flow liquid desiccant dehumidifier. Based on the contacting area estimation method addressed in a previous study, the effects of the geometrical parameters of a cross-flow liquid desiccant dehumidifier on dehumidification performance were analyzed via a numerical simulation. A series of simulations were conducted by adopting a two-dimensional heat and mass transfer numerical model suggested from previous literature (Liu et al., 2007). Based on the simulation process, the parametric analysis of the geometrical parameters on the dehumidification performance of a cross-flow dehumidifier were conducted. The dehumidifier tower configuration for achieving dehumidification performance comparable to that of the counter-flow liquid desiccant dehumidifier is proposed based on the parametric analysis results.

Simulation overview

Geometrical parameters for a cross-flow liquid desiccant dehumidifier

In a liquid desiccant dehumidifier, the dehumidification process occurs when the process air passes through packing media which is sufficiently wetted by the desiccant solution. During this process, dehumidification performance depends on the air-solution contact area and contact time. In a cross-flow dehumidifier, the desiccant solution is sprayed from the top of the packing media while the process air flows from the side of the packing media. This leads to the air side mass transfer area and the solution side mass transfer area being different, as shown in Figure 1.

To derive the configuration of a cross-flow liquid desiccant dehumidifier for improving the dehumidification performance, the effects of the geometrical parameters of a liquid desiccant dehumidifier on dehumidification performance were analyzed via a numerical simulation. In this study, the packing height, length, and width were considered as the key geometrical parameters. In addition, the aspect ratio of the air side, defined as the ratio of the packing width to height (Eq. 1), and the aspect ratio of the solution side, defined as the ratio of the packing length to width (Eq. 2), were also used as geometrical parameters.

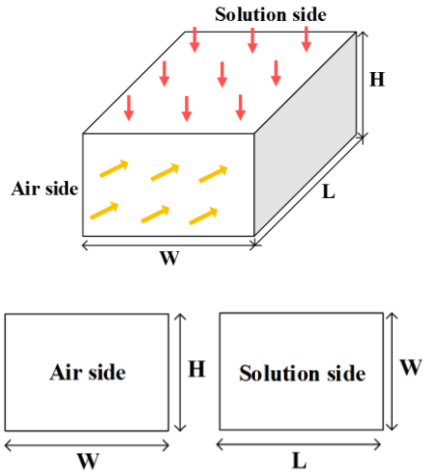

Figure 1: Schematic of air/solution side of a cross-flow liquid desiccant dehumidifier.

$$WH = \frac{W}{H} \quad (1)$$

$$\mathrm{LS} = \frac{L}{W} \quad (2)$$

Calculations of the contacting area

As shown in Equation 3, the air-desiccant contacting area is equal to the dehumidifier volume multiplied by the specific surface area per unit volume. The specific surface area per unit volume can be estimated using Equation 4−7. With Equation 4, the equivalent diameter of a flow channel in the packing media can be calculated with the given flow channel properties summarized in Table 1 (Al-Farayedhi et al., 2002). Given the equivalent diameter of a flow channel and its sheet thickness, the void fraction can be obtained using Equation 5. Then, the total available packing surface per unit volume (a_t) can be calculated using Equation 6.

$$a_w = V \cdot a_p \quad (3)$$

$$d_{eq} = B \cdot y[\frac{1}{2s} + \frac{1}{(2s+B)}] \quad (4)$$

$$e = 1 - \frac{4t}{d_{eq}} \quad (5)$$

$$a_t = \frac{4e}{d_{eq}} \quad (6)$$

According to a previous study, the heat and mass transfer between the air and desiccant solution is relatively more dependent on the solution flow rate than on the air flow rate (Al-Farayedhi et al., 2002). Therefore, the specific surface area can be estimated using Equation 7 when given the total available packing surface, and the solution superficial velocity which is equal to the solution flow rate divided by the solution side cross-sectional area.

$$a_p = a_t[1 - 1.203 \cdot (\frac{v_s^2}{s \cdot g})^{0.111}] \quad (7)$$

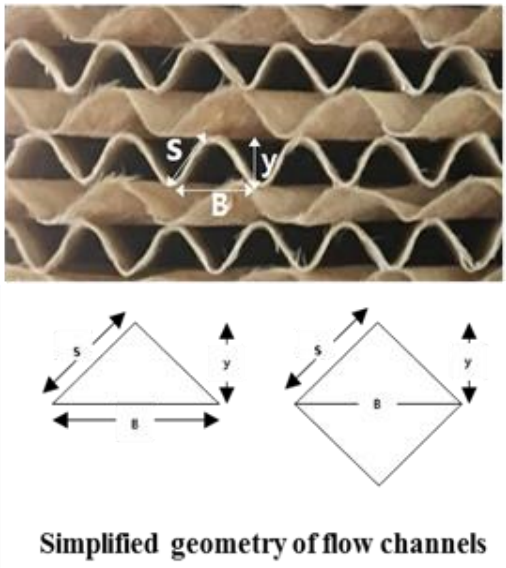

Figure 2: Channel geometry of the packing media.

Table 1: Properties of the packing channel.

Description	Contents
Flute height (y) [m]	0.007
Channel base (B) [m]	0.011
Channel side (s) [m]	0.0077
Sheet thickness (t) [m]	$2.28 \cdot 10^{(-4)}$

Theoretical analysis of dehumidification performance of a cross-flow dehumidifier

Previous studies have developed the numerical models for analyzing the dehumidification process in a cross-flow liquid desiccant dehumidifier. In this study, the numerical model is derived from partial differential equations for het and mass balance between process air and desiccant solution. In a cross-flow liquid desiccant dehumidifier, the heat and mass transfer process in the cross-flow type dehumidifier occurs not only in the solution flow direction (z-axis), from z = 0 to z = H, but also in the air flow direction (x-axis), from x = 0 to x = L. Because the process air and desiccant solution conditions, along with the dehumidifier width direction (y-axis) are uniform, it is assumed that the dehumidification process occurs only on the x-z plane as shown in Figure 3. Therefore, the differential elements of the x-z plane of the computational domain, which is discretized into M × N meshes, can be expressed as dx=L/M and dz=H/N. In this study, the domain was discretized into 20 nodes in the x- and z-directions. Other assumptions are as follows: adiabatic dehumidification process, the heat and mass transfer is equal to the specific surface area of the packing media, constant air flow rate, the heat and mass transfer are steady state.

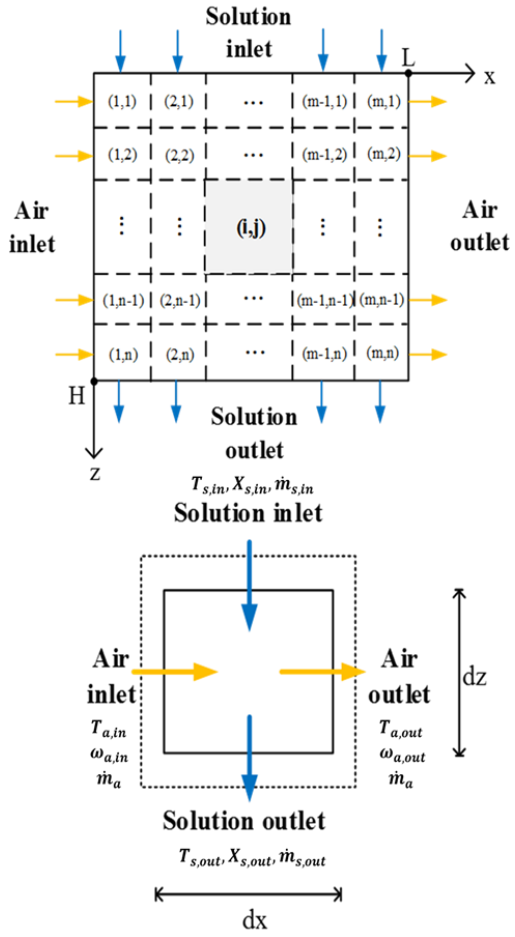

Figure 3: Schematic of heat and mass transfer process in a cross-flow dehumidifier (Liu et al., 2007).

$$\dot{m}_a \frac{\partial h_a}{\partial x} \cdot L + \frac{\partial (\dot{m}_s h_s)}{\partial z} \cdot H = 0 \quad (8)$$

$$\dot{m}_a \frac{\partial \omega_a}{\partial x} \cdot L + \frac{\partial \dot{m}_s}{\partial z} \cdot H = 0 \quad (9)$$

$$d(\dot{m}_s X_s) = 0 \quad (10)$$

The overall heat and mass and moisture transfer between the air and solution are as follows:

$$\frac{\partial h_a}{\partial x} = \frac{NTU_m \cdot Le}{L}\left[\left(h_{a,eq} - h_{a,in}\right) + \lambda_T\left(\frac{1}{Le} - 1\right) \times \left(\omega_{a,eq} - \omega_{a,in}\right)\right] \quad (11)$$

$$\frac{\partial \omega_a}{\partial x} = \frac{NTU_m}{L}\left(\omega_{a,eq} - \omega_{a,in}\right) \quad (12)$$

where the number of mass transfer unit (NTU_m) and Lewis number (Le) are defined in Equations 13 and 14, respectively.

$$NTU_m = \frac{h_m \cdot a_w}{\dot{m}_a} \quad (13)$$

$$Le = \frac{\alpha}{D_{ab}} \quad (14)$$

In this study, the mass transfer coefficient is expressed by the Sherwood (Sh) number. NTU_m can be rewritten in the form of the Sh number, as shown in Equation 15:

$$NTU_m = Sh \cdot \frac{\rho_a \cdot D_a \cdot a_w}{\dot{m}_a \cdot d_{eq}} \quad (15)$$

Equations 8−12 presented earlier can be solved with the boundary conditions, which are given as follows:

$$\begin{Bmatrix} (T_a)_{z=0} = T_{a,in} \\ (\omega_a)_{z=0} = \omega_{a,in} \\ (T_s)_{x=0} = T_{s,in} \\ (X_s)_{x=0} = X_{s,in} \\ (\dot{m}_s)_{x=0} = \dot{m}_{s,in} \end{Bmatrix} \quad (16)$$

Consequently, the gradients of the operating parameters: air temperature, air humidity ratio, solution temperature, solution concentration, and desiccant solution flow rate, can be calculated for each module of the cross-flow liquid desiccant dehumidifier.

Dehumidification performance index

In this study, the dehumidification effectiveness (ε_d) and pressure loss (ΔP) were adopted as a performance index of the liquid desiccant dehumidifier. The dehumidification effectiveness (ε_d) is defined as the ratio of the actual humidity ratio variation of the process air to the theoretical maximum humidity ratio variation (Eq. 17).

$$\varepsilon_d = \frac{\omega_{a,in} - \omega_{a,out}}{\omega_{a,in} - \omega_{a,eq}} \quad (17)$$

The equilibrium humidity ratio ($\omega_{a,eq}$) can be determined by using Equation 18 when the saturation vapor pressure of the solution (P_s) and the atmospheric pressures (P_a) are known. The saturation vapor pressure of the solution (P_s) at a given desiccant solution condition can be acquired by using the second-order polynomial (Eq. 19) suggested by Fumo and Goswami (2002) with the model coefficients shown in Table 2.

$$\omega_{a,eq} = 0.622 \frac{P_s}{P_a - P_s} \quad (18)$$

$$P_s = (\alpha_0 + \alpha_1 T_{s,in} + \alpha_2 T_{s,in}^2) + (\alpha_3 + \alpha_4 T_{s,in} + \alpha_5 T_{s,in}^2) X_{s,in} + (\alpha_6 + \alpha_7 T_{s,in} + \alpha_8 T_{s,in}^2) X_{s,in}^2 \quad (19)$$

Table 2: Model coefficients for the equation of saturation vapor pressure of the solution.

Model coefficients		
α_0	α_1	α_2
+4.5821	−0.1592	+0.0073
α_3	α_4	α_5
−18.3816	+0.5661	−0.0193
α_6	α_7	α_8
+21.3120	−0.6660	+0.0133

The pressure drop in a packed-bed liquid dehumidifier can be calculated by Equations 20 and 21. The constants C_1, C_2, and C_3 vary with packing type.

$$\Delta P = 0.125 f_0 \left(\frac{\rho_a V_a^2 a_w}{\varepsilon^{4.65}}\right) \quad (20)$$

$$f_0 = \frac{C_1}{Re_a} + \frac{C_2}{Re_a^{0.5}} + C_3 \quad (21)$$

Simulation results

Validation of mathematical model

In this study, the numerical model of a cross-flow liquid desiccant dehumidifier was adopted to analyze the effects of the changes of the dehumidifier physical dimensions on dehumidification performance. Lithium chloride (LiCl) solution was adopted as a desiccant solution, and *Sh* number was calculated by using empirical correlations suggested from previous experiment study (Cho et al., 2018). As shown in Equation 22, the empirical correlations predicting the *Sh* number is derived as a function of five operating parameters: inlet air temperature, inlet air humidity ratio, inlet solution temperature, inlet solution concentration, and air velocity. The model coefficients of the empirical correlations are summarized in Table 3.

$$Sh = \alpha_0 + \alpha_1 T_{a,in} + \alpha_2 \omega_{a,in} + \alpha_3 T_{s,in} + \alpha_4 X_{s,in} + \alpha_5 V_a + \alpha_6 (T_{a,in} \cdot X_{s,in}) + \alpha_7 (T_{a,in} \cdot V_a) + \alpha_8 (\omega_{a,in} \cdot T_{s,in}) + \alpha_9 (\omega_{a,in} \cdot X_{s,in}) + \alpha_{10} (\omega_{a,in} \cdot V_a) + \alpha_{11} (T_{s,in} \cdot X_{s,in}) + \alpha_{12} (T_{s,in} \cdot V_a) + \alpha_{13} (X_{s,in} \cdot V_a) \quad (22)$$

Table 3: Model coefficients for a cross-flow liquid desiccant dehumidifier.

Model coefficients		
α_0	α_1	α_2
+2.5573	- 0.0703	+0.0654
α_3	α_4	α_5
-0.0562	+6.7833	+1.3298
α_6	α_7	α_8
+0.1890	-0.0225	+0.0002
α_9	α_{10}	α_{11}
-0.1974	+ 0.0087	+0.1500
α_{12}	α_{13}	
-0.0133	+1.4163	

The proposed model was validated by comparison with experimental data from a previous study (Cho et al., 2018). As shown in Table 4, the operating ranges of the simulation conditions were set with consideration to the valid range of each operating parameter in the experiment, and the packing width, height and length were set as 0.35 m, 0.35 m, and 0.70 m, respectively.

Table 4: Operating ranges of the simulation conditions.

Operation parameter	Low	High
Inlet air temperature [°C]	26.90	34.40
Inlet air humidity ratio [g/kg]	10.19	22.51
Inlet solution temperature [°C]	14.31	32.34
Inlet solution concentration [%]	31.72	38.54
Air flow rate [kg/s]	0.064	0.169
Solution flow rate [kg/s]	0.159	0.169

Figure 4 shows the comparison of dehumidification effectiveness values predicted by the proposed model and the measurement data. Although the dehumidification effectiveness values predicted by the proposed model are slightly lower than those from the experimental data, the simulation results generally agreed well with the measurement data within 20% error bounds.

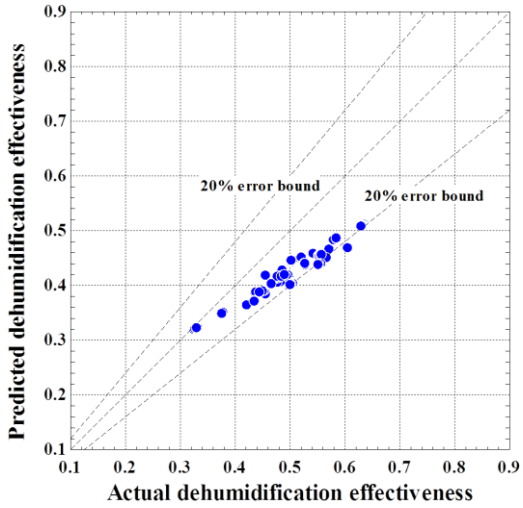

Figure 4: Comparison of the simulation results with experimental data.

Consequently, the comparison results indicate that the proposed correlation is applicable to predict dehumidification performance of the cross-flow type liquid desiccant dehumidifier.

Effects of the air/solution side mass transfer area on dehumidification performance

Using the proposed model, the effects of the air side and solution side mass transfer area on the dehumidification performance of a cross-flow liquid desiccant dehumidifier were analyzed. Regarding the simulation conditions of the six operating parameters: the inlet temperature and humidity ratio of the process air were set at 30.2 ºC and 20.3 g/kg based on local dehumidifier test standards (SAREK 202-2014); the inlet desiccant solution's temperature and concentration were set at 23.2 ºC and 34.9%;the mass flow rate of air and the mass flow rate of the desiccant solution were set at 0.169 kg/s; the initial dehumidifier size was set at 0.35 m width (W), 0.35 m height (H), and 0.70 m length (L). In the simulations performed for the sensitivity of air side mass transfer area, the packing width, height, and length were verified sequentially within the valid range while the six operating parameters were fixed to their initial values summarized as Table 5, and the aspect ratio of the solution side were set as 1. In the case of the solution side mass transfer area, the packing width, height, and length were changed within the valid range, while the operating parameters were fixed and the aspect ratio of the air side were set as 1.

Table 5: Operating values of the initial simulation conditions

Operation parameter	Value
Inlet air temperature [ºC]	30.2
Inlet air humidity ratio [g/kg]	20.3
Inlet solution temperature [ºC]	23.2
Inlet solution concentration [%]	34.9
Air flow rate [kg/s]	0.169
Solution flow rate [kg/s]	0.169

Figure 5 shows the dehumidification effectiveness in relation to changes in the aspect ratio of the air side and solution side of the cross-flow type dehumidifier. As shown in Figure 5, dehumidification effectiveness varied from 3.1 % to 88.3 % when the aspect ratio of the solution side was varied 0.1–10. In the case of the air side aspect ratio, dehumidification effectiveness values varied from 31.7 % to 54.1 %. These results indicate that the dehumidifier solution side has a significant influence on the dehumidification performance of a cross-flow type dehumidifier compared with changes to the dehumidifier air side. This superior influence is mainly because increasing air flow rate decreases dehumidification effectiveness owing to shorter contact time, although increasing the air/solution flow rate leads to increase in the mass transfer coefficient between the air and the solution. From the simulation results, it is clear that increasing the solution side aspect ratio has more impact on improving the dehumidification performance of a cross-flow liquid desiccant dehumidifier compared with increasing the air side aspect ratio.

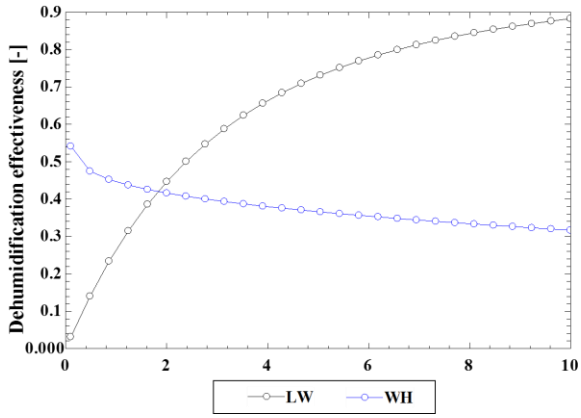

Figure 5: Effect of the air/solution side aspect ratio on dehumidification performance.

Effects of width/length on dehumidification performance

From the simulation results discussed earlier, one can see that the increase of the solution side mass transfer area in a cross-flow liquid desiccant dehumidifier achieves higher dehumidification performance than the increase of the air side mass transfer area. As shown in Equation 2, the solution side aspect ratio is defined as the ratio of the packing length to the packing width. To investigate a more effective way to derive the dehumidifier configuration for improving the dehumidification performance of a cross-flow liquid desiccant dehumidifier, the effects of the packing width and length on dehumidification performance of a cross-flow dehumidifier were analyzed.

Figures 6 shows the variations in the dehumidification effectiveness and pressure drop with the increase of the packing width. With the increase of the packing width change ratio (defined as the modified packing width to the initial packing width, from 0.5 to 2), the dehumidification effectiveness increases from 39.4% to 45.9%, while the pressure drop decreases from 25.11 Pa to 2.40 Pa. Also, when the packing width increases, the air superficial

velocity (V_a) decreases, which in turn decreases the *Sh* number and increases the pressure drop. However, the air-desiccant solution contacting area also increases owing to the increase of the packing volume. This effect counteracts the increase of the mass transfer coefficient (h_m), which leads to there being little change in dehumidification effectiveness.

Figure 7 shows the variations of the dehumidification effectiveness and the pressure drop with changes to the packing length. When the packing length change ratio (defined as the modified packing length to the initial packing length), was varied from 0.5 to 2, the dehumidification effectiveness and the pressure drop increased from 24.8% to 65.5%, and from 3.87 Pa to 15.07 Pa, respectively. This is because the increase in the packing length increases the mass transfer coefficient (h_m) owing to the increased air-desiccant contacting area, and the packing length also increases the pressure drop owing to the increase of the air flow path passing through the dehumidifier.

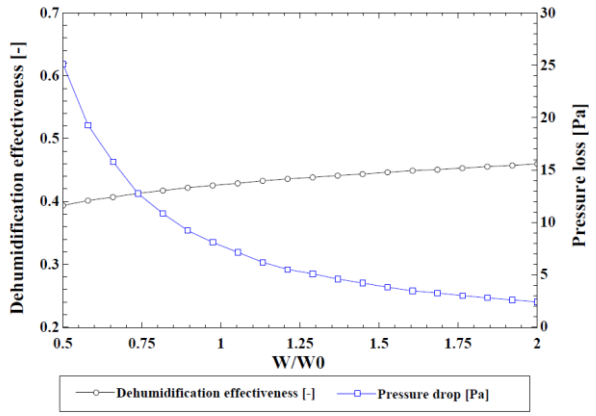

Figure 6: Effect of the dehumidifier width on dehumidification performance.

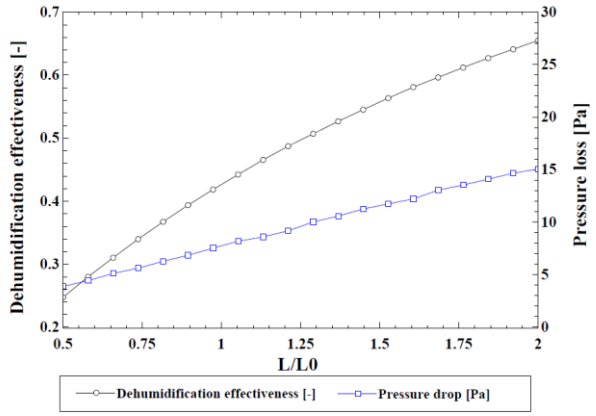

Figure 7: Effect of the dehumidifier length on dehumidification performance.

Discussion

As shown in the simulation results, it is clear that the solution side mass transfer area has a relatively more significant effect on the dehumidification performance of a cross-flow liquid desiccant dehumidifier. In addition, increasing the packing length achieves higher dehumidification effectiveness compared with increasing the packing width. To investigate the dehumidifier physical dimensions which achieve a dehumidification performance comparable to that of a counter-flow dehumidifier, the dehumidification performance of a counter-flow liquid desiccant dehumidifier and that of a cross-flow liquid desiccant dehumidifier were investigated with changes to the packing length change ratio via a series of simulation processes. The operating conditions are the same as shown in Table 5. The initial cross-flow dehumidifier size was set at 0.35 m width (W), 0.35 m height (H), and 0.70 m length (L). Likewise, the counter-flow dehumidifier size was set at 0.35 m width (W), 0.70 m height (H), and 0.35 m length (L).

Figure 8 compares the dehumidification effectiveness between the counter-flow and the cross-flow liquid desiccant dehumidifiers. When both counter-flow and cross-flow dehumidifiers of the same physical size operated in humid operating conditions, the dehumidification effectiveness in the counter-flow dehumidifier was 62.8 %, while that of the cross-flow dehumidifier was 44.6 %. As shown in Figure 8 however, the dehumidification effectiveness in a cross-flow dehumidifier steadily increases with the increase of the packing length change ratio. When the packing length is about 1.8 times the initial packing length, the cross-flow liquid desiccant dehumidifier achieves dehumidification performance equal to that of the counter-flow liquid desiccant dehumidifier.

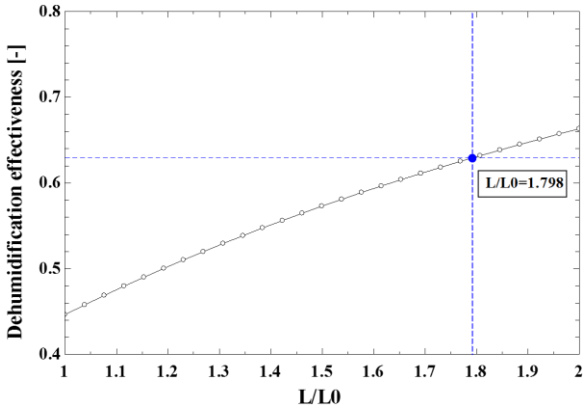

Figure 8: Comparison of dehumidification performance between counter-flow and cross-flow type dehumidifiers.

Conclusion

This study conducted the parametric analysis of each geometrical parameter on the dehumidification performance of a cross-flow liquid desiccant dehumidifier. One can see that the solution side mass transfer area has a more significant effect on the dehumidification performance than that of the air side. In addition, increasing the packing length achieves a more significant improvement to the dehumidification performance of a cross-flow dehumidifier compared with increasing the packing width. Consequently, it may be concluded that the dehumidification performance of a cross-flow liquid desiccant dehumidifier can be improved to be comparable with that of the counter-flow dehumidifier by modifying the physical dimensions of the packing tower, especially

by modifying the packing length. Further study is necessary to evaluate the entire operating performance (i.e., dehumidification performance and energy consumption) of a dimension-modified cross-flow dehumidifier when adopted in a liquid desiccant-assisted air conditioning system in building applications

Nomenclature

$\alpha_0 - \alpha_{13}$	Model coefficients
α	Thermal conductivity [m^2/s]
α_p	Effective interfacial area per unit volume [m^2/m^3]
α_t	Packing surface area per unit volume [m^2/m^3]
α_w	Air-solution wetting area [m^2]
B	Channel base [m]
$C_1 - C_3$	Model coefficients
D_{ab}	Mass conductivity [m^2/s]
d_{eq}	Equivalent diameter of packing channel [m]
e	Void fraction of packing media [-]
g	Gravitational constant [m/s]
h	Enthalpy [kJ/kg]
h_{fg}	Heat of water vaporization [kJ/kg]
h_m	Mass transfer coefficient [$kmol/m^2K$]
H	Packing height [m]
L	Packing length [m]
Le	Lewis number [-]
L/G	Liquid to gas ratio [-]
LW	Solution-side aspect ratio [-]
$\dot{m}$	Mass flow rate [kg/s]
NTU_m	Number of mass transfer unit [-]
ΔP	Pressure loss [Pa]
P_a	Water-vapor partial pressure [Pa]
P_s	Saturation vapor pressure of desiccant solution [Pa]
s	Channel side [m]
Sh	Sherwood number [-]
t	Packing sheet thickness [m]
T	Temperature [°C]
u	Velocity [m/s]
V	Packing volume [m^3]
W	Packing width [m]
	Solution concentration [-]
y	Flute height [m]

Greek symbols

ε	Effectiveness [-]
ω	Humidity ratio of humid air [kg/kg_a]

Subscripts

a	Air
deh	Dehumidification
eq	Equilibrium
in	Inlet
ini	Initial
out	Outlet
sol	Desiccant solution
w	Water vapor

Acknowledgement

This work was supported by the Korean Agency for Infrastructure Technology Advancement (KAIA) grants (19CTAP-C141826-02), by the Korean Institute of Energy Technology Evaluation and Planning (KETEP) (No. 20184010201710), and by the National Research Foundation of Korea (NRF) grant (No.2019R1A2C2002514).

References

Al-Farayedhi AA, Gandhidasan P. (2002). Evaluation of heat and mass transfer coefficients in a gauze-type structured packing air dehumidifier operating with liquid. *International Journal of Refrigeration (25)*, 330–339.

Cho H-J, Park J, Kim B-J, Jeong J-W. (2018). Dehumidification performance comparison of counter/cross flow type liquid desiccant dehumidifiers. *Proceedings of SAREK Conference*. Seoul (Korea), 248-251, November 2018.

Fu HX, Liu XH. (2017). Review of the impact of liquid desiccant dehumidification on indoor air quality. *Building and Environment (116)*, 158–172.

Fumo N, Goswami DY. (2002). Study of an aqueous lithium chloride desiccant system: Air dehumidification and desiccant regeneration. *Solar Energy (72)*, 351–361.

Liu XH, Jiang Y, Qu KY. (2007). Heat and mass transfer model of cross flow liquid desiccant air dehumidifier/regenerator. *Energy conversation and management (48)*, 546–554.

SAREK Standard (2014). Method of Testing for Rating Desiccant Dehumidifiers Utilizing Heat for the Regeneration Process. *The Society of Air-conditioning and Refrigerating Engineers of Korea* (SAREK) (SAREK 202-2014